
Sound Explanation for Trustworthy Machine Learning (Extended Abstract)

Kai Jia

*Department of Electrical Engineering and Computer Science,
Massachusetts Institute of Technology*

jiakai@mit.edu

Pasapol Saowakon

*Department of Electrical Engineering and Computer Science,
Massachusetts Institute of Technology*

zoomswk@mit.edu

Limor Appelbaum

Beth Israel Deaconess Medical Center

lappelb1@bidmc.harvard.edu

Martin Rinard

*Department of Electrical Engineering and Computer Science,
Massachusetts Institute of Technology*

rinard@csail.mit.edu

Abstract

We take a formal approach to the explainability problem of machine learning systems. We argue against the practice of interpreting black-box models via attributing scores to input components due to inherently conflicting goals of attribution-based interpretation. We prove that no attribution algorithm satisfies specificity, additivity, completeness, and baseline invariance. We then formalize the concept, sound explanation, that has been informally adopted in prior work. A sound explanation entails providing sufficient information to causally explain the predictions made by a system. Finally, we present the application of feature selection as a sound explanation for cancer prediction models to cultivate trust among clinicians.

1 Introduction

As machine learning systems take more essential roles in decision making in critical situations, there is increasing focus on understanding the reasoning mechanism of the learned models (Molnar, 2020). Prior work has attempted to interpret black-box models in a post hoc manner (Ribeiro et al., 2016; Zeiler & Fergus, 2014; Sundararajan et al., 2017), train models that generate explanations besides predictions (Park et al., 2018; Kumar et al., 2022), or build inherently interpretable models (Andrews et al., 1995; Sudjianto & Zhang, 2021).

However, there is no consensus on choosing the best interpretation algorithm if the model is not inherently interpretable. The evaluation of post hoc or self-explaining interpretation methods is often subjective (Doshi-Velez & Kim, 2017); there are systematic differences in how human individuals approach decision making based on model interpretation (Broniatowski et al., 2021). Different interpretation algorithms can generate different results for practical applications, while practitioners do not seem to have a principled way to resolve those differences (Krishna et al., 2022).

This paper argues that the above difficulties in designing and evaluating interpretation algorithms partially arise from fundamentally conflicting objectives of interpretability. In particular, we show that no attribution algorithm for black-box models possesses all the following desirable properties: specificity (unused inputs have a zero score), additivity (attribution scores decompose over model addition), completeness (attribution

completely explains model output), and baseline invariance (rank of inputs is invariant to change of baseline inputs).

Instead of pursuing other post hoc interpretation methods, we advocate an alternative route towards model explainability. We formalize the concept of *sound explanation*. Briefly speaking, a sound explanation is a subset of the information used by a machine learning system, perceived as understandable by humans, that causally determines the system’s output. A sound explanation is always accurate and reliable in explaining how the system makes a prediction. The challenge faced by system designers is how to design conceptually understandable explanations. For example, a decision tree is a sound explanation; however, a tree with thousands of variables and hundreds of levels is hardly a satisfactory explanation to any human. The idea of sound explanation has been informally adopted by prior work. Rudin (2019) argues that black-box models should be abandoned in favor of inherently interpretable models, which naturally provide sound explanations. Koh et al. (2020) proposes models with concept bottlenecks, which is a type of sound explanation. Unlike prior work, our research formally defines sound explanation instead of using heuristic arguments.

We present a case in cancer prediction. We provide sound explanation via feature selection on large datasets derived from Electronic Health Records (EHRs) containing millions of patients and thousands of features. We design an efficient algorithm for feature selection for neural networks. The final model is then trained on the less than 100 selected features. We work with two cancer types: Pancreatic Ductal Adenocarcinoma (PDAC, a common type of pancreatic cancer) and Hepatocellular Carcinoma (HCC, a common type of liver cancer). The selected features agree well with known PDAC and HCC risk factors, thus providing confidence in our models among clinicians.

2 Nonexistence of Ideal Interpretation

This section considers a restricted form of interpretation that assigns an importance score to each dimension of any given input relative to a fixed baseline input. Such a score attribution formulation is closely related to cost sharing that has been extensively studied in game theory. We follow the notations of Friedman (2004) and Sundararajan et al. (2017) to establish our results.

Definition 2.1 (Interpretation). Let $F : \mathbb{R}^n \mapsto [0, 1]$ be a continuously differentiable function, $\mathbf{x}' \in \mathbb{R}^n$ be a baseline input, and $\mathbf{x} \in \mathbb{R}^n$ be an arbitrary input. An interpretation is a function $A : (\mathbb{R}^n \mapsto [0, 1]) \times \mathbb{R}^n \times \mathbb{R}^n \mapsto \mathbb{R}^n$ such that $A(\mathbf{x}; F, \mathbf{x}') = (a_1, \dots, a_n)$ with $a_i \in \mathbb{R}$ being the contribution of x_i towards the value of $F(\mathbf{x}) - F(\mathbf{x}')$. For simplicity of notations, we define $A_i(\mathbf{x}; F, \mathbf{x}') \stackrel{\text{def}}{=} a_i$. We call the value of $A(\mathbf{x}; F, \mathbf{x}')$ an attribution of $F(\mathbf{x})$ to \mathbf{x} relative to a baseline input \mathbf{x}' .

Here F is the function of interest, such as a deep neural network. A baseline input is an uninformative input that typically satisfies $F(\mathbf{x}') = 0$, such as a black image for image classification tasks, as suggested by Sundararajan et al. (2017). Given an input \mathbf{x} , an interpretation assigns importance scores to individual components of \mathbf{x} to explain the prediction $F(\mathbf{x})$.

We now define the properties that an ideal interpretation should have.

Specificity An interpretation should be specific to influential inputs: it should assign zero scores to inputs that do not influence function values. An interpretation without specificity may be adversarially manipulated by adding unused inputs. Specificity is called “dummy” in Friedman (2004) and “sensitivity(b)” in Sundararajan et al. (2017).

Definition 2.2 (Specificity). An interpretation A satisfies specificity if for any function F and integer $i \in [1, n]$ such that $\forall \mathbf{x} \in \mathbb{R}^n, \delta \in \mathbb{R} : F(\mathbf{x}) = F(\mathbf{x} + \delta \mathbb{1}_i)$ where $\mathbb{1}_i$ is all zero but one at the i^{th} dimension, then $A_i(\mathbf{x}; F, \mathbf{x}') = 0$.

Additivity An interpretation is additive if its attribution decomposes over function addition. Additivity is a weak and natural constraint on the behavior of interpretation.

Definition 2.3 (Additivity). An interpretation A satisfies additivity if for any F_1 and F_2 , $A(\mathbf{x}; F_1 + F_2, \mathbf{x}') = A(\mathbf{x}; F_1, \mathbf{x}') + A(\mathbf{x}; F_2, \mathbf{x}')$.

Completeness An interpretation is complete if its attribution explains all of the output. Completeness is also called efficiency in the cost sharing literature (Friedman, 2004).

Definition 2.4 (Completeness). An interpretation A satisfies completeness if $\sum_{i=1}^n A_i(\mathbf{x}; F, \mathbf{x}') = F(\mathbf{x}) - F(\mathbf{x}')$.

Baseline invariance The above properties have been studied by prior work. We propose a new property, *baseline invariance*. A baseline-invariant interpretation generates the same rank of inputs for different choices of \mathbf{x}' . Baseline invariance is preferable because the widely used choice of $\mathbf{x}' = \mathbf{0}$ (Sundararajan et al., 2017) is arbitrary. For example, for image classification tasks, it is equally sensible to set $\mathbf{x}' = \mathbf{0}$ as a black image, $\mathbf{x}' = \mathbf{1}$ as a white image, $\mathbf{x}' = \mathbf{0.5}$ as a gray image, $\mathbf{x}' = E_{\mathbf{x} \sim D} \mathbf{x}$ as the mean of training data, or $\mathbf{x}' \sim N$ according to some noise distribution N . An ideal interpretation should give similar attributions for different choices of baseline inputs.

Definition 2.5 (Baseline invariance). An interpretation A satisfies baseline invariance if for any baseline inputs $\mathbf{x}'_1 \in \mathbb{R}^n$ and $\mathbf{x}'_2 \in \mathbb{R}^n$ and any function F such that $F(\mathbf{x}'_1) = F(\mathbf{x}'_2)$, it holds that for any indices i and j , $A_i(\mathbf{x}; F, \mathbf{x}'_1) < A_j(\mathbf{x}; F, \mathbf{x}'_1)$ iff $A_i(\mathbf{x}; F, \mathbf{x}'_2) < A_j(\mathbf{x}; F, \mathbf{x}'_2)$.

Theorem 2.6. *There is no interpretation A satisfying all of these properties: specificity, additivity, completeness, and baseline invariance.*

Our proof depends on the path method. The path method is a class of interpretation methods that integrate the gradients of F along a path. They satisfy specificity, additivity, and completeness (Friedman & Moulin, 1999).

Definition 2.7 (Path method). Given a continuous path function $\gamma : [0, 1] \mapsto \mathbb{R}^n$ such that $\gamma(0) = \mathbf{x}'$ and $\gamma(1) = \mathbf{x}$, the path method $A^\gamma(\mathbf{x}; F, \mathbf{x}')$ computes the attribution as

$$A_i^\gamma(\mathbf{x}; F, \mathbf{x}') \stackrel{\text{def}}{=} \int_{t=0}^1 \partial_i F(\gamma(t)) d\gamma(t) \quad (1)$$

Proof of Theorem 2.6. Assume A satisfies specificity, additivity, and completeness. We prove that A is inconsistent with baseline invariance. Friedman (2004, Theorem 1) implies that given \mathbf{x} and \mathbf{x}' , A can be decomposed as a convex combination of path methods. Here it suffices to consider a single path method. Consider a linear function on \mathbb{R}^2 : $F(\mathbf{x}) = x_1 - x_2$, two baseline inputs $\mathbf{x}'_1 = (-1, -1)$ and $\mathbf{x}'_2 = (1, 1)$, and the input $\mathbf{x}_t = (1, 0)$. For two path functions γ_1 and γ_2 such that $\gamma_1(0) = \mathbf{x}'_1$, $\gamma_2(0) = \mathbf{x}'_2$, and $\gamma_1(1) = \gamma_2(1) = \mathbf{x}_t$, their attributions are $A^{\gamma_1}(\mathbf{x}_t; F, \mathbf{x}'_1) = (2, -1)$ and $A^{\gamma_2}(\mathbf{x}_t; F, \mathbf{x}'_2) = (0, 1)$ (following (1)), which violates baseline invariance as the ranks of x_{t1} and x_{t2} in the two attributions switch. \square

3 Sound Explanation

A sound explanation of a machine learning system should accurately and reliably describe how the system makes a prediction. This work considers the problem of explaining the system’s prediction given a single input. A central part of our definition is to include all the critical information used by the system as a sound explanation. The information presentation should be in a human-understandable way, but we do not attempt to define or quantify what is understandable by humans. After achieving soundness, one can trade off between explainability (i.e., how easy the explanation is to understand, which typically relates to the complexity of the explanation) and prediction accuracy.

For example, consider the task of pancreatic cancer risk prediction given a person’s health records. Assume a two-step system with two black-box models A and B . Model A takes the raw health records of a patient and outputs values indicating the presence or absence of a few meaningful concepts, such as abdominal pain, personal history of cancer, and abnormal lab results. Model B calculates the risk score only using the output of A . The output of A is a sound explanation of the system because one can verify that the system is not using any information other than the presented explanation to make the prediction.

This research does not consider the faithfulness of a sound explanation. A sound explanation may fail to match the claimed semantics. In the above example, the system can claim that a person has a higher

pancreatic cancer risk due to recent onset of abdominal pain. However, the presence of abdominal pain is a prediction by another model, which may be incorrect from the original medical records.

Formally, we represent a machine learning system \mathcal{M} as a computational graph $\mathcal{M} = (G, P)$, where $G = (V, E)$ is a directed acyclic graph and P is a map from vertices to computable functions. Decompose $V = I \cup \{t\} \cup U$, where I represents the input variables, t the output variable, and U the set of internal computation steps. Each non-input vertex $v \in V \setminus I$ has an associated computable function P_v defining its functionality. (Only) Vertices in I have no incoming edges, and (only) t has no outgoing edges. Let x be an input to the system, which is a map from a variable $v \in I$ to its value, denoted as x_v . Define a value function $f_x(\cdot)$ for the vertices. For $v \in I$, $f_x(v) = x_v$. For other vertices $v \in V \setminus I$, $f_x(v)$ is recursively computed as $f_x(v) = P_v(f_x(i) : (i, v) \in E)$ where P_v is the computable function associated with v . The output of \mathcal{M} on input x is $f_x(t)$.

Definition 3.1 (Sound explanation). For a machine learning system $\mathcal{M} = (G = (V = I \cup \{t\} \cup U, E), P)$, a sound explanation is a cut $C = (S, T)$ such that $I \subseteq S$, $t \in T$, $S \cap T = \emptyset$, and $S \cup T = V$.

Define $V_C \stackrel{\text{def}}{=} \{v \in S \mid \exists v' \in T : (v, v') \in E\}$ as the set of vertices at the boundary of the cut. Given an input x , define

$$\mathfrak{X}_x \stackrel{\text{def}}{=} \{(v, f_x(v)) \mid v \in V_C\}$$

The information in \mathfrak{X}_x is presented to a human as the explanation of $f_x(t)$ on the input x .

The design space of sound explanations is how to decompose a machine learning system into a computational graph and a cut so that the explanation \mathfrak{X} is meaningful to humans.

Our formulation incorporates inherently interpretable models. For example, for a decision tree, a typical sound explanation is to present all the branching decisions of the tree. In our framework, this can be implemented by converting the tree into a computational graph where each tree node corresponds to a graph vertex. Add edges to connect input variables to internal tree nodes. Add an output node t with incoming edges from all the leaf nodes. For a non-input node v , $f_x(v) \in \{0, 1\}$ indicates whether this node is activated by the input x . The sound explanation is the cut $C = (V \setminus \{t\}, \{t\})$. The explanation \mathfrak{X}_x shows which leaf node is activated for x , corresponding to a path on the tree.

4 An Example: Cancer Prediction

We demonstrate sound explanation of models for cancer prediction. We work with two cancer types: Pancreatic Ductal Adenocarcinoma (PDAC) and Hepatocellular Carcinoma (HCC). Our datasets have thousands of features per patient with millions of patients. Neural networks trained on the full dataset perform well, but clinicians are reluctant to trust those models because even a linear model with thousands of inputs is difficult to understand. We designed a scalable and effective feature selection algorithm that resulted in 83 features for PDAC and 86 features for HCC without a significant performance drop. The selected features, which can be formulated as a binary mask on the input in a computational graph per Definition 3.1, serve as a sound explanation. Since the lists of selected features correspond well to known PDAC and HCC risk factors, clinicians gain higher confidence in our models.

4.1 Task and Datasets

We formulate cancer prediction as a binary classification task. Given the Electronic Health Records (EHRs) of a patient and a cutoff date, the model predicts risk of cancer diagnosis 6 to 18 months after the cutoff date from EHR entries up to the cutoff date.

We derived our datasets from EHRs obtained on a federated network platform. The platform aggregates EHRs from nearly 60 Healthcare Organizations (HCOs) in the United States. EHRs have date-indexed entries of diagnosis, medication, and lab records as well as demographic information including sex, birth year, and race for each patient. To protect privacy, patients are anonymized, and dates are perturbed. Data can only be accessed and processed within a secure computer network.

For each type of cancer, we queried the platform for patients with certain International Classification of Diseases (ICD) diagnosis codes to construct the positive set and sampled patients without those ICD codes to construct the negative set. For PDAC we used ICD-10 codes C25.0, C25.1, C25.2, C25.3, C25.7, C25.8, and C25.9 and ICD-9 code 157. For HCC we used ICD-10 code C22.0 and ICD-9 code 155.0. We filtered the EHR data to improve data quality; for example, we removed patients with entries two months after their recorded death date. To compute the features, we filtered diagnosis, medication, and lab codes by keeping those that appear in at least 1% of the patients in the positive set. We derived a fixed-length feature vector for each patient by calculating features such as first date, last date, frequency, time span, medication frequency, and lab value for each code. Our features also include age, sex, and frequency of clinical encounters. All features except frequency of clinical encounters have a corresponding binary existence feature to account for missing data. Our PDAC dataset has 63,884 positive cases and 3,604,863 negative cases with 5427 features. Our HCC dataset has 49,380 positive cases and 1,094,011 negative cases with 5610 features. The features are sparse. On average, each feature has a 94% chance of being zero.

4.2 Method

For each positive patient, we sampled a cutoff date uniformly 6 to 18 months before their diagnosis date. For negative patients, we sampled cutoff dates matched with the distribution of cutoff dates of positive patients. We derived fixed-length features for each patient based on EHR entries up to the sampled cutoff date. The cutoff dates were resampled for each minibatch during training.

We trained MLP neural networks with two hidden layers, each having 64 and 20 neurons with tanh nonlinearity, respectively. We applied L_0 regularization to the weights to improve model generalizability. We extended the BinMask method (Jia & Rinard, 2023) to select features: we applied L_0 regularization to a parameterized binary input mask and obtained a feature mask by comparing the smoothed mask with a threshold of 0.5. We then iteratively removed features selected by BinMask. At each iteration, we evaluated the AUCs on the training set with each feature removed and removed the feature that resulted in the lowest AUC drop. This process was repeated until the AUC was 0.006 lower than the AUC obtained before feature removal. We retrained the networks from random initialization using the selected features.

4.3 Results

On the PDAC dataset, the model with all 5427 features achieved 0.834 (95% CI: 0.828 to 0.839) AUC. BinMask selected 121 features. Iterative feature removal kept 83 features. The final model achieved 0.826 (95% CI: 0.820 to 0.831) AUC. Features include known PDAC risk factors such as age, sex, diabetes mellitus, pancreatitis, pancreatic cysts, abdominal pain, and smoking (Principe & Rana, 2020), as well as novel features associated with hypertension, hypercholesterolemia, kidney function, and frequency of clinical visits.

On the HCC dataset, the model with all 5610 features achieved 0.926 (95% CI: 0.921 to 0.930) AUC. BinMask selected 147 features. Iterative feature removal kept 86 features. The final model achieved 0.922 (95% CI: 0.917 to 0.926) AUC. Features include known HCC risk factors such as cirrhosis, hepatitis, smoking, alcohol, age, and sex (Yang et al., 2019). The model also utilizes features associated with Nonalcoholic Fatty Liver Disease (NAFLD), the most common cause of HCC developing in a non-cirrhotic liver (Gawrieh et al., 2019). NAFLD-related features include obesity, diabetes mellitus, hypertension, and dyslipidemia, which correlate with the metabolic syndrome (Kim et al., 2018). The features suggest that the model may predict HCC cases that develop in a NAFLD liver, without underlying cirrhosis.

Appendix A presents the complete lists of selected features.

References

- Robert Andrews, Joachim Diederich, and Alan B Tickle. Survey and critique of techniques for extracting rules from trained artificial neural networks. *Knowledge-based systems*, 8(6):373–389, 1995.
- David A Broniatowski et al. Psychological foundations of explainability and interpretability in artificial intelligence. *NIST, Tech. Rep*, 2021.

-
- Finale Doshi-Velez and Been Kim. Towards a rigorous science of interpretable machine learning. *arXiv preprint arXiv:1702.08608*, 2017.
- Eric Friedman and Herve Moulin. Three methods to share joint costs or surplus. *Journal of economic Theory*, 87(2):275–312, 1999.
- Eric J Friedman. Paths and consistency in additive cost sharing. *International Journal of Game Theory*, 32: 501–518, 2004.
- Samer Gawrieh, Lara Dakhoul, Ethan Miller, Andrew Scanga, Andrew DeLemos, Carla Kettler, Heather Burney, Hao Liu, Hamzah Abu-Sbeih, Naga Chalasani, et al. Characteristics, aetiologies and trends of hepatocellular carcinoma in patients without cirrhosis: a united states multicentre study. *Alimentary pharmacology & therapeutics*, 50(7):809–821, 2019.
- Kai Jia and Martin Rinard. Effective neural network l_0 regularization with binmask. *arXiv preprint arXiv:2304.11237*, 2023.
- Donghee Kim, Alexis Touros, and W Ray Kim. Nonalcoholic fatty liver disease and metabolic syndrome. *Clinics in liver disease*, 22(1):133–140, 2018.
- Pang Wei Koh, Thao Nguyen, Yew Siang Tang, Stephen Mussmann, Emma Pierson, Been Kim, and Percy Liang. Concept bottleneck models. In *International Conference on Machine Learning*, pp. 5338–5348. PMLR, 2020.
- Satyapriya Krishna, Tessa Han, Alex Gu, Javin Pombra, Shahin Jabbari, Steven Wu, and Himabindu Lakkaraju. The disagreement problem in explainable machine learning: A practitioner’s perspective. *arXiv preprint arXiv:2202.01602*, 2022.
- Sayantana Kumar, Sean C Yu, Thomas Kannampallil, Zachary Abrams, Andrew Michelson, and Philip RO Payne. Self-explaining neural network with concept-based explanations for icu mortality prediction. In *Proceedings of the 13th ACM International Conference on Bioinformatics, Computational Biology and Health Informatics*, pp. 1–9, 2022.
- Christoph Molnar. *Interpretable machine learning*. Independently published, 2020.
- Dong Huk Park, Lisa Anne Hendricks, Zeynep Akata, Anna Rohrbach, Bernt Schiele, Trevor Darrell, and Marcus Rohrbach. Multimodal explanations: Justifying decisions and pointing to the evidence. In *Proceedings of the IEEE conference on computer vision and pattern recognition*, pp. 8779–8788, 2018.
- Daniel R Principe and Ajay Rana. Updated risk factors to inform early pancreatic cancer screening and identify high risk patients. *Cancer letters*, 485:56–65, 2020.
- Marco Tulio Ribeiro, Sameer Singh, and Carlos Guestrin. "why should i trust you?" explaining the predictions of any classifier. In *Proceedings of the 22nd ACM SIGKDD international conference on knowledge discovery and data mining*, pp. 1135–1144, 2016.
- Cynthia Rudin. Stop explaining black box machine learning models for high stakes decisions and use interpretable models instead. *Nature machine intelligence*, 1(5):206–215, 2019.
- Agus Sudjianto and Aijun Zhang. Designing inherently interpretable machine learning models. *arXiv preprint arXiv:2111.01743*, 2021.
- Mukund Sundararajan, Ankur Taly, and Qiqi Yan. Axiomatic attribution for deep networks. In *International conference on machine learning*, pp. 3319–3328. PMLR, 2017.
- Ju Dong Yang, Pierre Hainaut, Gregory J Gores, Amina Amadou, Amelie Plymoth, and Lewis R Roberts. A global view of hepatocellular carcinoma: trends, risk, prevention and management. *Nature reviews Gastroenterology & hepatology*, 16(10):589–604, 2019.
- Matthew D Zeiler and Rob Fergus. Visualizing and understanding convolutional networks. In *Computer Vision—ECCV 2014: 13th European Conference, Zurich, Switzerland, September 6–12, 2014, Proceedings, Part I 13*, pp. 818–833. Springer, 2014.

A Complete lists of selected features for cancer prediction

This section presents the complete lists of selected features. We define a heuristic score, the *univariate model AUC*, to rank the features. The univariate model AUC represents the predictive power of a single feature on the test set. It is computed by evaluating the model AUC on the test set with values of each feature while setting all other features to zero. Figure 1 presents the list of PDAC features, and Figure 2 presents the list of HCC features. In the plots, the label **diag** refers to diagnosis features, **med** to medication features, and **lab** to lab features. Letters in the brackets indicate the types of derived features: **e** for existence, **fd** for first date, **ld** for last date, **p** for time span, **f** for frequency, **v** for latest lab value, **ve** for whether a valid lab value exists, **s** for lab value slope, and **se** for whether lab value slope can be computed.



Figure 1: List of selected features ranked by univariate model AUC for PDAC

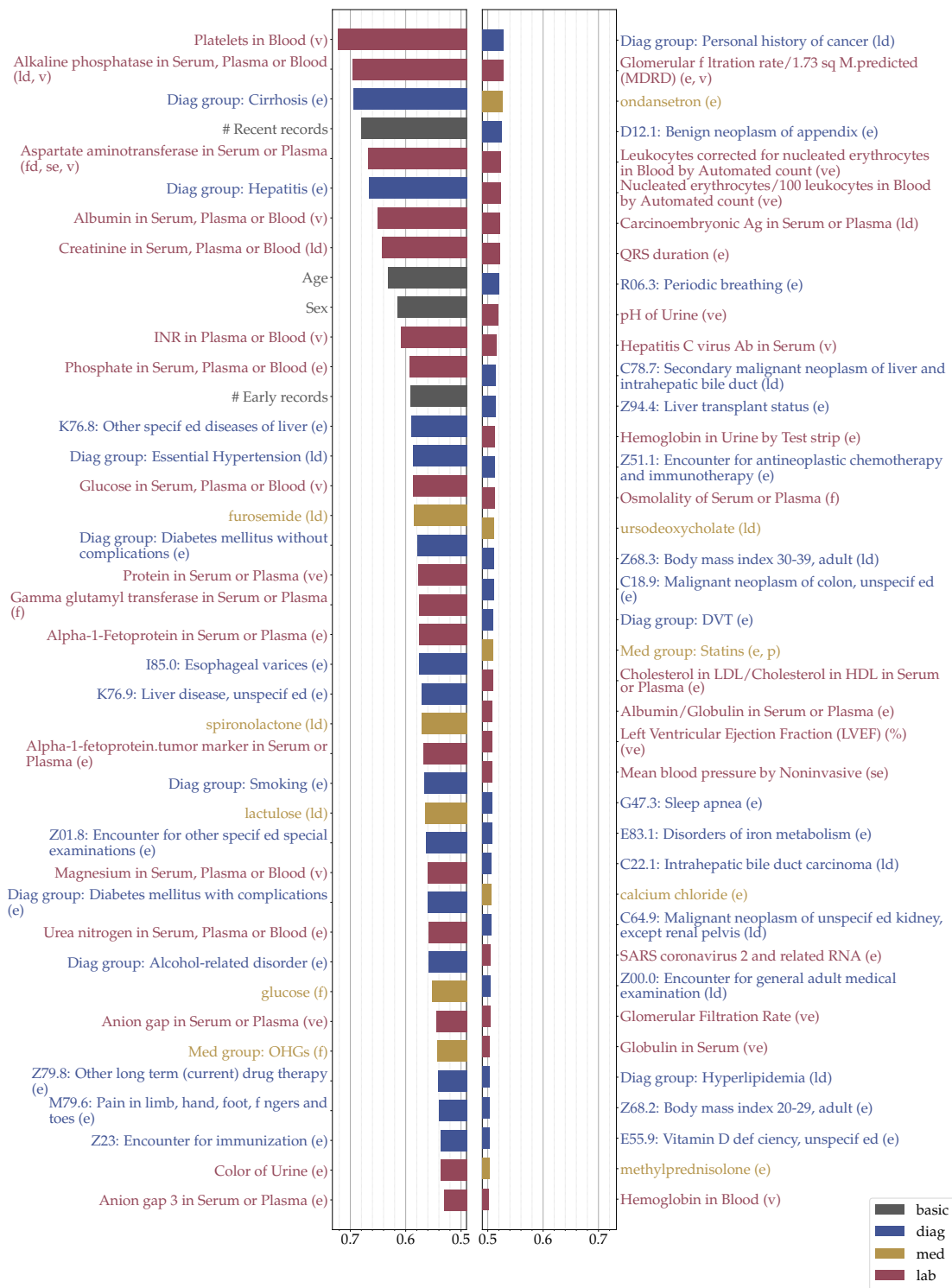


Figure 2: List of selected features ranked by univariate model AUC for HCC